Journal of Structural Biology 195 (2016) 11–18

Contents lists available at ScienceDirect

Journal of Structural Biology

journal homepage: www.elsevier.com/locate/yjsbi

Structure of USP7 catalytic domain and three Ubl-domains reveals a connector α-helix with regulatory role

Robbert Q. Kim, Willem J. van Dijk, Titia K. Sixma *

Division of Biochemistry and Cancer Genomics Center, Netherlands Cancer Institute, Plesmanlaan 121, 1066 CX Amsterdam, The Netherlands

ARTICLE INFO

Article history:
Received 17 February 2016
Received in revised form 12 May 2016
Accepted 13 May 2016
Available online 13 May 2016

Keywords:
Ubiquitin conjugation
Deubiquitination
USP7
Helix stability

ABSTRACT

Ubiquitin conjugation is an important signal in cellular pathways, changing the fate of a target protein, by degradation, relocalisation or complex formation. These signals are balanced by deubiquitinating enzymes (DUBs), which antagonize ubiquitination of specific protein substrates.

Because ubiquitination pathways are critically important, DUB activity is often carefully controlled. USP7 is a highly abundant DUB with numerous targets that plays complex roles in diverse pathways, including DNA regulation, p53 stress response and endosomal protein recycling. Full-length USP7 switches between an inactive and an active state, tuned by the positioning of 5 Ubl folds in the C-terminal HUBL domain. The active state requires interaction between the last two Ubls ($USP7^{45}$) and the catalytic domain ($USP7^{CD}$), and this can be promoted by allosteric interaction from the first 3 Ubl domains of USP7 ($USP7^{123}$) interacting with GMPS.

Here we study the transition between USP7 states. We provide a crystal structure of $USP7^{CD123}$ and show that CD and Ubl123 are connected via an extended charged alpha helix. Mutational analysis is used to determine whether the charge and rigidity of this 'connector helix' are important for full USP7 activity.

1. Introduction

The covalent attachment of ubiquitin (Ub) to lysines of target proteins is an important post-translational modification (Hershko and Ciechanover, 1998; Varshavsky, 2012) that is carried out by a cascade of E1 activating enzymes, E2 conjugating enzymes and E3 ligases (Passmore and Barford, 2004; Pickart, 2001; Streich and Lima, 2014). Apart from mono-ubiquitination, ubiquitin can form chains, by further ubiquitination on any of its seven lysines or the N-terminus (Komander and Rape, 2012). Different ubiquitination states, either mono-ubiquitination or different types of poly-ubiquitination, will have different signalling outcomes for the target protein; ranging from cellular location to proteasomal degradation (Hicke and Dunn, 2003; Shabek and Ciechanover, 2010).

To reverse the ubiquitination, deubiquitinating enzymes (DUBs) can hydrolyse the bond between ubiquitin and the target lysine (Clague et al., 2013; Komander et al., 2009). Besides functions in ubiquitin processing and at the proteasome, DUBs can antagonise the ubiquitination step and affect the cellular fate of the target protein (Clague et al., 2012). Dysfunction of DUBs can cause an imbalance in cells and therefore DUBs play important roles in infectious diseases, cancer and neurological diseases (Hussain et al., 2009; Nanduri et al., 2013; Todi and Paulson, 2011).

DUBs are specialized isopeptidases that hydrolyse the ubiquitin bond. In the human genome about 80 different DUBs have been identified providing specificity for different targets (Nijman et al., 2005; Clague et al., 2012). These are divided into five classes, based on their catalytic domain (CD) architecture. Next to this class defining catalytic domain, DUBs may have a series of regulatory domains (Reyes-Turcu et al., 2009). These extra domains can confer substrate specificity, by recruiting the target, but may also influence the overall activity of the DUB (Sahtoe and Sixma, 2015).

USP7, or HAUSP (Everett et al., 1997), is one of the first DUBs identified and remains one of the best studied ones (Holowaty et al., 2003; Wrigley et al., 2011). USP7 is involved in many pathways as it deubiquitinates a wide range of targets. It functions in apoptosis and senescence through its deubiquitinating activity in the p53 pathway, primarily affecting MDM2 (Brooks and Gu, 2006; Cummins et al., 2004), but also p53 (Li et al., 2002) and TSPYL5 (Epping et al., 2011). It acts on a large number of targets in chromatin and DNA regulation, such as H2B (van der Knaap et al., 2005), Chk1 (Alonso-de Vega et al., 2014), Claspin (Faustrup et al., 2009), UVSSA (Schwertman et al., 2013), SCML2 (Lecona et al., 2015), DNMT1 (Du et al., 2010), BRCA1-A (Sowa et al., 2009) and RNF168 (Zhu et al., 2015), but also interacts with FOXO4 (van der Horst et al., 2006), PTEN (Song et al., 2008),

* Corresponding author.
E-mail address: t.sixma@nki.nl (T.K. Sixma).

http://dx.doi.org/10.1016/j.jsb.2016.05.005
1047-8477/

MAGE-L2 (Hao et al., 2015), GMPS (van der Knaap et al., 2005) and viral proteins like ICP0 and EBNA-1 (Holowaty and Frappier, 2004), making it an interesting but complex protein to study.

USP7 belongs to the family of ubiquitin specific proteases (USP), which have a papain-like catalytic domain (CD, denoted as USP7^{CD}) (Hu et al., 2002). USP7 is one of the larger USP family members with an N-terminal TRAF domain (Fig. 1a), which is critical for recruitment of its targets like p53 or MDM2 (Saridakis et al., 2005; Sheng et al., 2006), and on the C-terminal side five ubiquitin-like (Ubl) domains. These five Ubl domains together are dubbed HUBL (for HAUSP-Ubl) domain and denoted as USP7^{12345}. Interestingly, proteins like GMPS, DNMT1 (Cheng et al., 2015) and ICP0 (Holowaty et al., 2003; Pfoh et al., 2015) interact primarily with Ubl12, while others like MDM2 and p53 (Ma et al., 2010) seem to have a secondary binding site here, showing that different types of interaction and regulation may occur.

Structural analysis has revealed that the *apo* structure of USP7^{CD} has a catalytic triad that is not functional, as the distance between active site residues is too large (Hu et al., 2002). In the presence of a covalently bound ubiquitin aldehyde, the catalytic triad is rearranged to generate a catalytically competent state of CD (Hu et al., 2002). Interestingly, for full activity the C-terminal domains are required, as the CD on its own showed a hundred-fold decrease in activity compared to full-length or the USP7^{CD12345} (Fernández-Montalván et al., 2007).

Faesen et al. showed that USP7 exists in an equilibrium between the active and inactive state and that the active state requires the presence of the Ubl45 domain. Ubl45 can bind to the USP7^{CD}, which then promotes the interaction between a C-terminal peptide on Ubl45 that causes a rearrangement of the switching loop on CD and induces the rearrangement of the catalytic triad into an active state (Faesen et al., 2011). The equilibrium between the active and

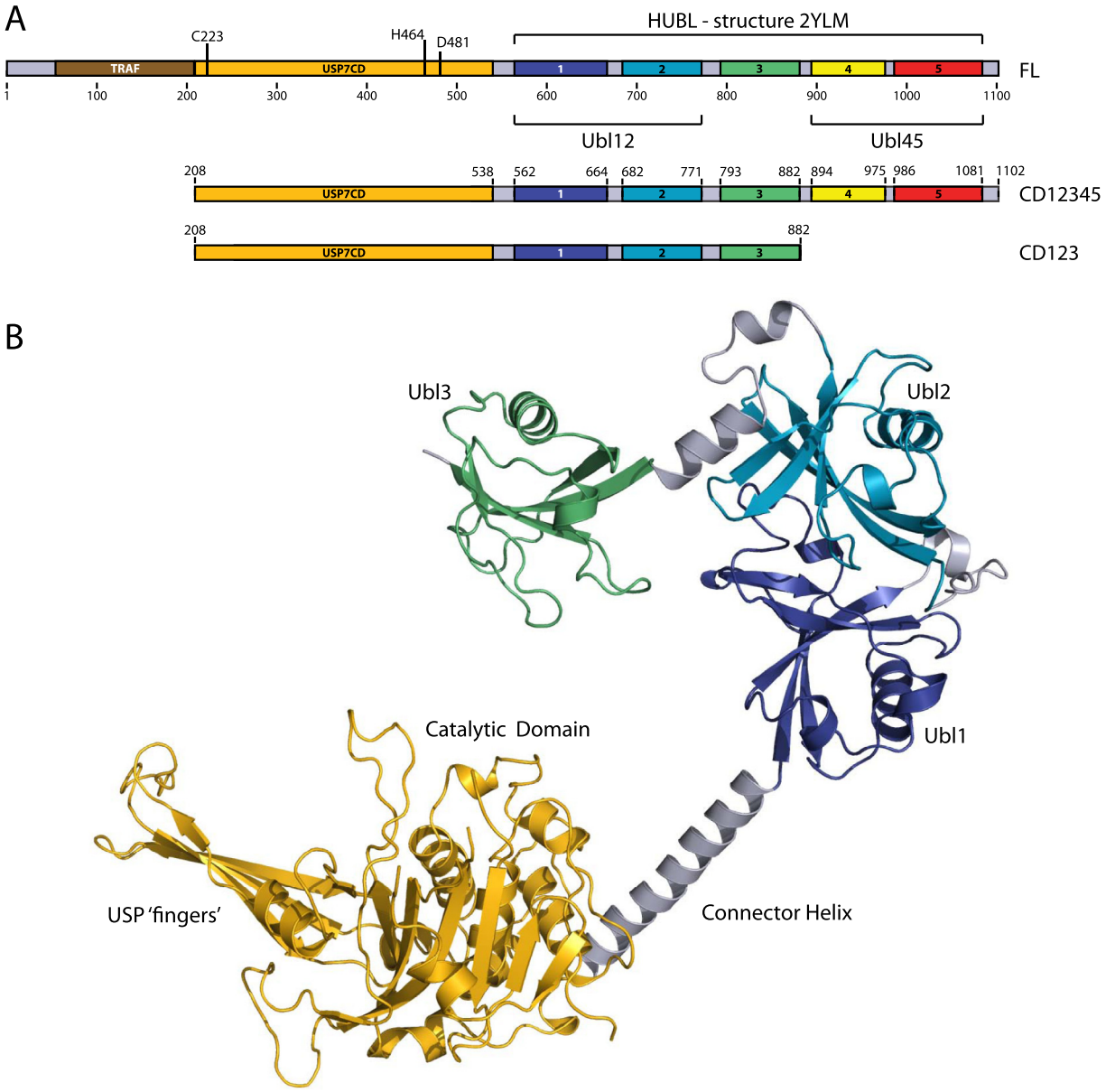

Fig. 1. The crystal structure of USP7^{CD123}. (a) Schematic overview of USP7 domains and constructs used. Also indicated are the catalytic residues and domain boundaries. The 'connector' helix, spanning from residue 538–562, is here defined as the full α-helix, stemming from the CD. The other domain boundaries are based on previously solved structures. Domain colours are used for all structural representation of USP7^{CD123}. (b) The crystal structure of USP7^{CD123} reveals a curved architecture of domains and a 'connector' α-helix that links the CD to Ubl1.

inactive state can be modulated further by the binding of the allosteric activator GMPS (van der Knaap et al., 2005). This protein binds to Ubl123 but promotes the interaction between CD and Ubl45, thus shifting USP7 towards the active side of the equilibrium.

Structural studies have shown that the Ubl domains are arranged in a 2-1-2 fashion (Faesen et al., 2011). The crystal structure of the full HUBL domain showed that the 5 Ubl domains can exist in an extended state, but geometrical restraints indicate that this domain needs to rearrange to enable interaction with the CD. This conclusion was supported by SAXS and binding data. Since the first two (Ubl12) and last two (Ubl45) Ubl domains are connected to Ubl3 by small linkers, some flexibility between the domains was proposed. However, how this 'folding back' is achieved is not clear and structures are required that show the arrangement of these domains relative to the CD.

Here we present a crystal structure of USP7^{CD123} containing the CD and the Ubl domains 1, 2 and 3. It shows that the catalytic domain is connected to the HUBL domain through a 26 amino-acid α-helical linker. This apparently rigid linker shows how the first three Ubl domains are positioned relative to the catalytic domain. We studied the role of this connecting element in positioning of the C-terminal domains and were able to show that the rigidity, length and charges on this linker may affect the activity of USP7.

2. Materials and methods

2.1. Constructs and mutations

USP7 constructs USP7^{CD123} (residues 208–882) and USP7^{CD12345} (res. 208–1102) were cloned into expression vector pGEX-6P-1 (GE Healthcare) using BamHI and NotI restriction sites based on the codon-optimised USP7 from Faesen et al., 2011. Mutations were introduced in USP7^{CD12345} using site-directed mutagenesis with overhanging primers.

2.2. Protein expression and purification

USP7 constructs were expressed in *Escherichia coli* BL21(DE3) T^{1R} cells using auto-induction medium overnight at 18 °C (Studier, 2005). Cells were pelleted and resuspended in lysis buffer (50 mM HEPES pH7.5; 250 mM NaCl; 1 mM EDTA; 1 mM DTT). DNAseI and 0.1 mM PMSF were added prior to lysis using Emulsiflex. The lysate was cleared by centrifuging at 20 k G and supernatant was applied to Glutathione Sepharose 4B beads (GE Healthcare). After washing the beads, the protein was eluted using 15 mM reduced glutathione and subjected to cleavage using 3C protease and dialysis versus 10 mM HEPES pH7.5, 50 mM NaCl, 1 mM EDTA, 1 mM DTT. Anion exchange on a PorosQ column (GE Healthcare) was performed using a salt gradient (50–500 mM NaCl; 10 mM HEPES pH7.5; 1 mM DTT). Protein fractions were pooled and concentrated, followed by size exclusion chromatography on a Superdex 200 column (GE Healthcare) equilibrated against 10 mM HEPES pH7.5; 100 mM NaCl; 1 mM DTT. If necessary, a GST FF column (GE Healthcare) was attached to the end of the gel filtration column to remove residual GST. The peak fractions were analysed by SDS-PAGE and pooled accordingly. Proteins were concentrated to 10 mg mL^{-1} for assays and up to 25 mg mL^{-1} for crystallization purposes. Generally, 1 L of culture yields 2 mg of purified protein.

2.3. Crystallization and data collection

USP7^{CD123} was used at a concentration of 25 mg mL^{-1} in a sitting drop vapour diffusion experiment using 96-well plates at 4 °C. Crystallization plates were set up using Mosquito (TTP Labtech) with 0.1 μL of mother liquor (15% PEG-3350; 0.2 M Sodium citrate pH ~ 8.5) and 0.1 μL of protein solution. Crystals appeared within one week and were flash-frozen in liquid nitrogen after being cryo-protected in mother liquor supplemented with 20% ethylene glycol.

X-ray diffraction data could be obtained from a single crystal to 3.4 Å on beamline ID 14-1 at the ESRF, Grenoble, France. The crystal belongs to space group F222 and the data were processed using XDS (Kabsch, 2010), yielding statistics shown in Table 1.

2.4. Structure determination

The structure of USP7^{CD123} was solved by molecular replacement using *PHASER* (McCoy et al., 2007) with search models for the catalytic domain (PDB code 1NB8; (Hu et al., 2002)) and the Ubl-domains (2YLM; (Faesen et al., 2011)), split into separate searches for Ubl12 and Ubl3. The separate solutions were merged to one monomer in the asymmetric unit. In the resulting electron density map, the connector helix could be built manually using *COOT* (Emsley et al., 2010). The resulting structure was refined, using *PROSMART* geometric restraints from the higher resolution reference structures (Nicholls et al., 2014), in iterative cycles of maximum-likelihood restrained refinement in *REFMAC* from the *CCP4* suite (Murshudov et al., 2011; Winn et al., 2011). The model was further validated and optimised using *MolProbity* (Davis et al., 2004) and *PDB_REDO* (Joosten et al., 2014). The final model had R_{work} and R_{free} values of 22.2% and 26.7% respectively.

2.5. Enzyme activity assays

The DUB activity of the USP7 variants was monitored by measuring the increase in fluorescence upon release of the Rhodamine

Table 1
Data processing and refinement statistics for the crystal structure of USP7^{CD123}.

USP7^{CD123}	
PDB accession code	
Space group	F222
Cell dimensions	
a (Å)	115.18
b (Å)	195.04
c (Å)	219.78
α (°)	90
β (°)	90
γ (°)	90
Monomers in ASU	1
Resolution (Å)	48.76–3.40
Outer shell (Å)	3.67–3.40
Beamline	ESRF ID14-1
Wavelength (Å)	0.97935
Observed reflections	77,295 (15,487)
Unique reflections	17,198 (3504)
R_{merge}	0.061 (0.733)
Multiplicity	4.5 (4.5)
Completeness	99.9 (100)
Mean (I/σ(I))	13.4 (1.9)
N° of protein atoms	5352
R_{work} (%)	22.2
R_{free} (%)	26.7
RMSD from ideality	
Bond lengths (Å)	0.008
Bond angles (°)	1.278
Chiral volume (Å^3)	0.071
Ramachandran plot	
Favoured (%)	634 (96%)
Disallowed (%)	3 (0%)
Average B-values (Å^2)	104.0

Values within parentheses are for the outer resolution shell.

fluorophore from quenched substrate Ub-Rho (UbiQ) using Pherastar plate reader (BMG LABTECH GmbH, Germany), with excitation wavelength 485 nm (±10 nm) and emission at 520 nm (±10 nm). For Michaelis-Menten analysis, 1 nM enzyme was used to react with concentrations of substrate as indicated. The initial rates were plotted against substrate concentration and fitted with a Michaelis-Menten model using non-linear regression in Prism 6 (GraphPad). These experiments were performed in triplicate on two different batches of protein.

2.6. Molecular weight determination using MALLS

Purified proteins were run on analytical gel filtration coupled to Multi-angle Laser Light Scattering (MALLS) detector MiniDawn Tristar (Wyatt Technologies, USA). Molecular weights of corresponding peaks were determined with refractive index using manufacturer's software (ASTRA).

2.7. Melting temperature assessment

Stability of wild type protein and mutants was tested using the Optim 1000 (Avacta, now Unchained Labs, USA). Using an excitation wavelength of 266 nm, scattering at 266 nm and fluorescence intensity over the spectrum between 300 nm and 400 nm were measured and analysed as function of the temperature using the manufacturer's software. Barycentric fluorescence curves were plotted using Prism 6 (GraphPad) and used to obtain melting temperatures.

3. Results

3.1. USP7^{CD123} crystal structure

We were able to express and purify a USP7 construct comprising residues 208-882. This construct contains the catalytic domain (CD) and the first three Ubl domains, from here on referred to as USP7^{CD123} (Fig. 1a). We obtained single crystals in a vapour diffusion setup at 4 °C with mother liquor of pH > 7, containing multivalent acids. During optimisation sodium citrate was found to yield the best diffracting crystals, resulting in a dataset diffracting to 3.4 Å (Table 1). The crystal belonged to space group F222 with unit cell parameters a = 115.2, b = 195.0 and c = 219.8 Å, with a rather high solvent content (68%) for a single monomer of 79 kDa (Table 1). The structure was solved by molecular replacement using *apo* USP7-CD (1NB8; Hu et al., 2002) followed by separate searches for Ubl12 and Ubl3 (2YLM; Faesen et al., 2011). After manual building of the connector helix, the model could be refined to R-values of R_{work} = 0.22 and R_{free} = 0.27 with good geometry (Table 1). The R-values are relatively good for a structure at this resolution, probably thanks to the external restraints generated by ProSmart from the higher resolution search models (Nicholls et al., 2014).

The failure of molecular replacement using Ubl123 from the previous structure as a whole, already indicates a conformational change in USP7^{CD123} with respect to the crystal structure of the extended HUBL (2YLM; Faesen et al., 2011). Indeed, the structural model for USP7^{CD123} shows the four domains in a curved, crescent-shaped conformation, where Ubl3 'bends' inwards, back to the catalytic domain (Fig. 1b). This backward bending contrasts with the extended conformation of the HUBL domain, and results in a globular overall shape for USP7^{CD123}.

3.2. Structural analysis of USP7^{CD123}

As shown previously USP7^{CD123} has the low activity that was observed for the catalytic domain alone (Fig. 2b; Faesen et al., 2011). Accordingly, we observe that the catalytic triad is misaligned, with the active-site cysteine and histidine separated by more than 10 Å (Fig. 2a). The catalytic domain aligns much better with the *apo* structure of USP7^{CD} (1NB8; Hu et al., 2002) separately (RMSD 0.53 Å on 322 Cα's) than with the activated ubiquitin-bound USP7^{CD} (1NBF; Hu et al., 2002) (RMSD 1.34 Å on 314 Cα's). The main differences with the *apo* structure are in a series of loops, that could not be modelled confidently in this low resolution structure, and the relatively poor density in the β-strands of

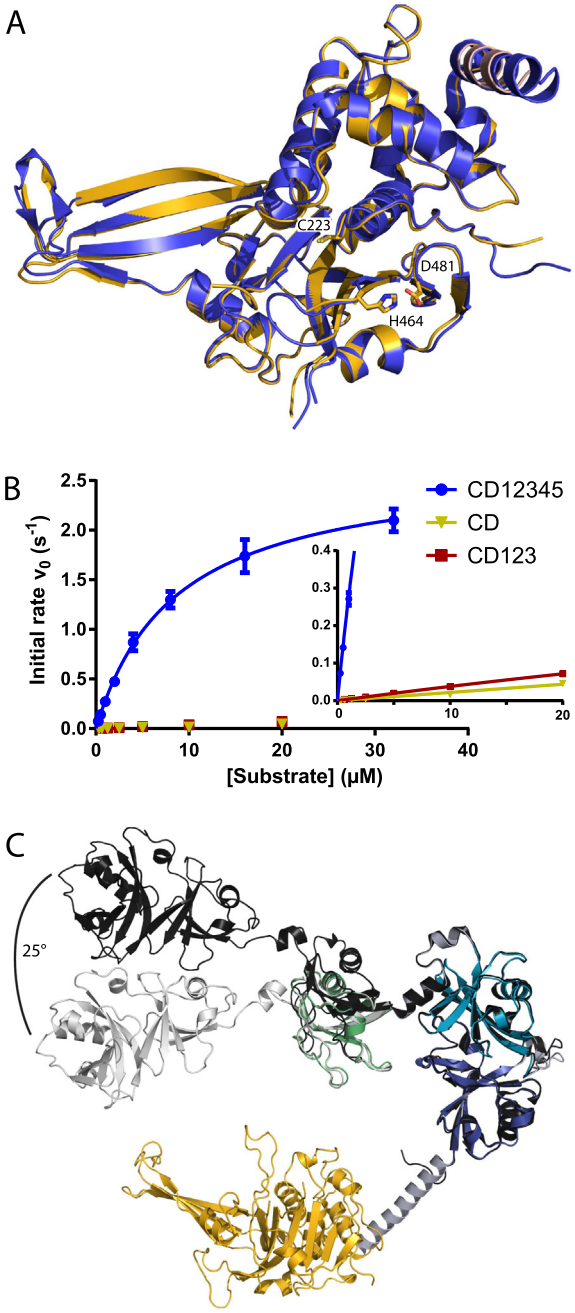

Fig. 2. Comparison of USP7^{CD123} to USP7 variants. (a) Structural alignment of the *apo* structure of USP7^{CD} (purple) and USP7^{CD} of USP7^{CD123} (gold) yields an RMSD of 0.53 Å. Both have the misaligned catalytic triad, confirming their inactive state. (b) Michaelis-Menten analysis of enzyme activities on minimal substrate Ub-Rho, comparing USP7^{CD12345} with USP7^{CD} and USP7^{CD123} shows that Ubl45 is necessary for full activity of USP7. Insert is a magnification of the larger figure. (c) Superposition of the HUBL structure (2YLM) on either Ubl12 (dark grey) or Ubl3 (light grey) of the USP7^{CD123} structure. The structural alignment shows an angle of 25°, emanating between Ubl2 and Ubl3.

the fingers region, which is mobile in other USP structures (see e.g. Clerici et al., 2014).

The overall arrangement of the Ubl123 is different from that observed in the extended state structure of the five Ubl domains (Fig. 2c, 2YLM; Faesen et al., 2011). When aligning the first two Ubls, the third Ubl shows a 25° rotation with respect to the extended structure (Fig. 2c). Such an angle was also observed in the co-crystal structures of Ubl123 with an ICP0-peptide (Pfoh et al., 2015) and the structure of HUBL with DNMT1 (Cheng et al., 2015). Both these structures could exhibit this rotation as consequence of binding of the protein partner, but the USP7^{CD123} structure shows that the protein alone can have this flexibility.

The bending of Ubl3 fits with the model proposed (Faesen et al., 2011), as this curving lessens the gap between the CD and the very C-terminus, reducing the distance between K882, the last residue of the construct crystallized, and C223, the active site, to 47 Å. In this gap, the remaining Ubl45 domain of 45 Å would fit perfectly (Fig. 2c), keeping in mind the extending, activating C-terminal peptide. As proposed earlier (Pfoh et al., 2015), this distance could be further bridged by a hinge motion at the region between Ubl3 and Ubl4, an area notoriously flexible, as seen in the full-length degradation pattern (results not shown and Faesen et al., 2011).

3.3. USP7^{CD} is connected to the Ubl domains by an α-helix

A new finding in the USP7^{CD123} crystal structure is the long α-helix connecting the catalytic domain to the Ubl domains (Fig. 1b). Previous structures have shown parts of the helix (Hu et al., 2002; Pfoh et al., 2015), and the structure of USP7^{CD123} confirms these helical fragments. This 39 Å helix (26 residues) connects the CD to the HUBL domains, and will be referred to as 'connector helix' from here onwards. The density for this part of the protein is relatively well-defined, most probably thanks to crystal packing and the rigidity in the element. Having two domains connecting over such a length with a rigid α-helical element could imply that the helix has an important function in the protein. Therefore we analysed whether this connector helix was important for activity.

3.4. The connector helix is necessary for full USP7 activity

First we studied whether the rigid extended nature of the connector is important for activity. The connector helix' rigidity can influence the correct positioning, because such an extended element will create distance between the CD and Ubl1. This distance could be necessary to position the activating C-terminal tail correctly for folding back onto the catalytic domain and promoting its activation. In order to investigate the role of the helix, we introduced two 'bending motifs' by mutating stretches AQK552 and EAH560 (Fig. 3a) to proline-glycine-proline in the USP7^{CD12345} construct, which contains the full HUBL domain.

These USP7^{CD12345} mutants could be expressed and purified according to the wild type protocol, although both mutants eluted later from the gel filtration column (Supplementary Fig. 1a). The wild type construct dimerises at concentrations above 1 mg/mL, and with the introduced mutations the dimerization equilibrium seems to have shifted to higher concentrations (Supplementary Fig. 1b). Furthermore, melting temperature analysis (Supplementary Fig. 1c) was performed, resulting in similar values, indicating the mutants are as stable as wild type protein.

Both AQK552PGP and EAH560PGP were analysed in a deubiquitination assay and compared to wildtype USP7^{CD12345} (Fig. 3b). The K_M values were similar, but the k_{cat} rates showed interesting differences (Table 2). The mutant with the bend at the end of the connector helix (EAH560PGP) exhibited similar activity as wildtype. This would indicate that the HUBL domain has enough intrinsic flexibility to overcome such a bending disruption at the end of the extending connector helix. In contrast, the mutant with a bend in the middle of the helix (AQK552PGP) has lower activity, due to a lower k_{cat} (Table 2, Fig. 3b). The increased flexibility within the helix may have changed the spatial location of the Ubl domains with respect to the CD and this could explain why the activation by Ubl45 is affected.

3.5. A charged patch in the connector helix has influence on USP7 activity

We identified a cluster of charged residues in the connector helix (K554, R555 and R558) all pointing inwards, towards the catalytic domain. On the complementary surface of the catalytic domain a similar positive cluster of five lysines was identified (Fig. 3c). These positive surfaces (with distances between 4 Å and 10 Å) could repel the connector helix away from the catalytic domain. We wondered if this would be relevant for the activity of USP7.

We made mutations in the active USP7^{CD12345} construct that neutralised (KR554AA R558A) or reverted (KR554AE R558E) the charge on the linker. These could be expressed and purified in a similar fashion as wild type USP7^{CD12345} (Supplementary Fig. 1a), indicating no drastic changes in fold. When comparing the mutants with wild type protein in a deubiquitination assay (Fig. 3b), they showed reduced activity, indicating that the charge has a role in the activity of USP7. The K_M-values are similar for the mutants and wild type, indicating that these mutants do not affect the binding of ubiquitin (Table 2). The values for k_{cat} are two-fold lower, which suggests that the charged patch influences the efficiency of the Ubl45 domain activation of the CD.

3.6. The connector helix has a minimum length to allow for full activity

Next to the helix' rigidity and charged patch, the length could influence the positioning of Ubl45, and thereby the activation. Therefore, we investigated the length of the connector and its effect on the activity of the USP7^{CD12345} construct. To this end we removed one or two α-helical turns (4 residues per turn) on the C-terminal (Δ561-564 and Δ557-564) as well as the N-terminal part (Δ538-541 and Δ538-545) of the helix (Fig. 3e).

These mutants could be expressed and purified using the USP7^{CD12345} protocol and the gel filtration profiles indicated a monomeric species (Supplementary Fig. 1a). The activity assays yielded similar K_M-values, however the activity of the mutants differed in k_{cat} (Fig. 3f and Table 2), indicating that the effect is not on the final positioning, but on the efficiency of reaching this stage. In agreement with the findings for the mutant EAH560PGP, where the last helical turn is affected, deletion of one turn does not affect catalysis. Deletion of a second turn, whether at the start or the end of the helix, affects the activity as shown by the two-fold lower values k_{cat}.

4. Discussion and conclusions

The large number of important targets reported for USP7 indicates that it has a number of separately regulated functions in the human cell, but its exact molecular functioning remains elusive. Here we present a partial structure of USP7, which shows how previously solved crystal structures are connected and allows near full-length modelling. The crystal structure reveals a long extended α-helix that connects the CD to the HUBL domain. We studied the importance of this connector helix and found that it may play in a role in regulation of activity by positioning the C-terminal element.

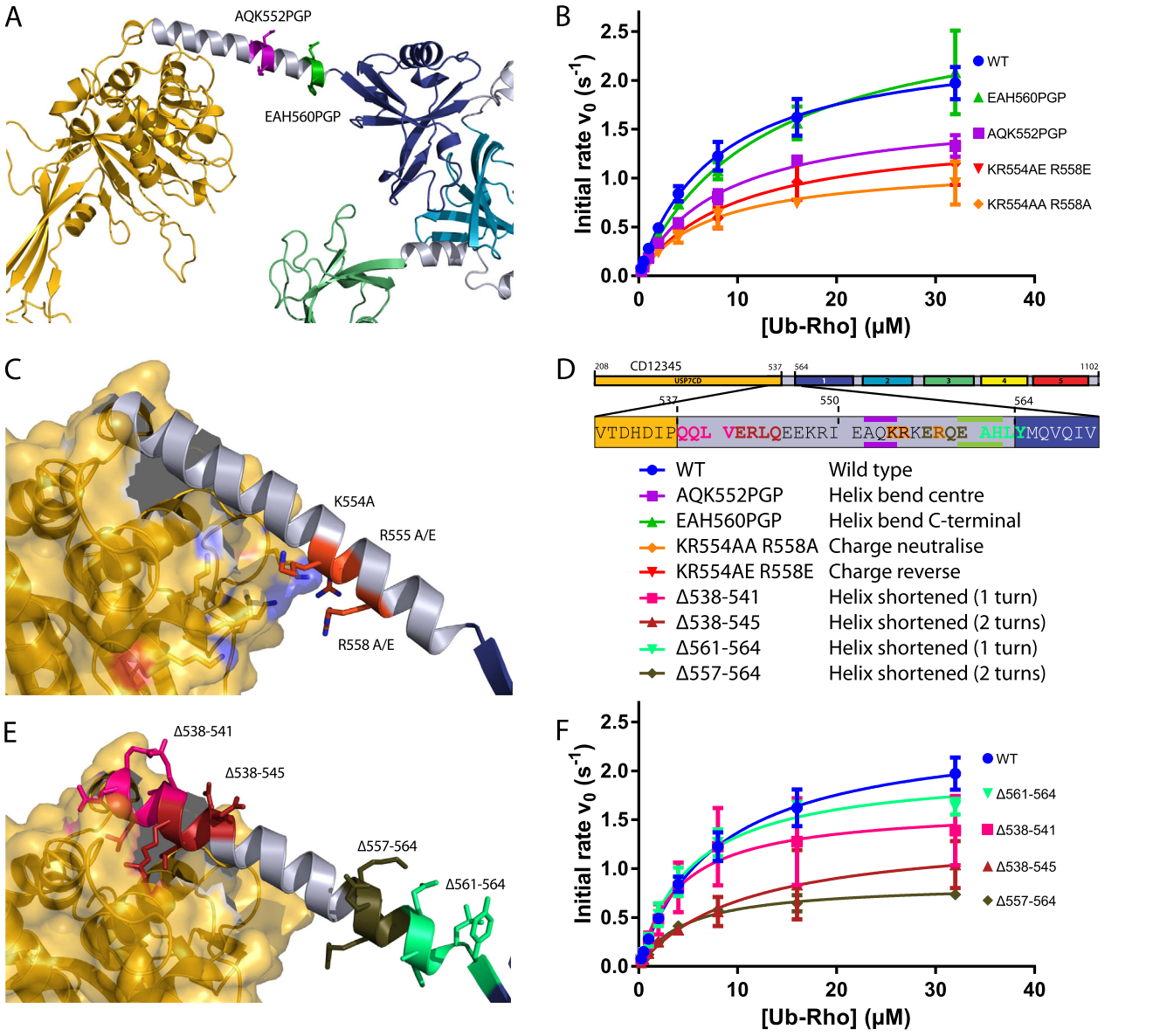

Fig. 3. The connector helix is important for full activity of USP7. (a) Mutations in the connector helix that affect its rigidity were introduced in two locations AQK552PGP (purple) and EAH560PGP (green). (b) Michaelis menten analysis of mutants that affect the charge or bending of the helix show similar K_M-values as wild type USP7^{CD12345}, but yield differences in k_{cat}. Curve colours are matched throughout the panels as indicated in Fig. 3d. (c) Mutations in the connector helix that affect a charged patch were introduced. Zoom in on the connector helix and surroundings shows a charged patch on both the connector helix and the CD. (d) Overview of the mutants made, serving as a legend to all panels in Fig. 3. (e) Zoom in on the connector helix, showing the deleted helix turns on its N-terminal end (red and pink) and the C-terminal end (shades of green). (f) Michaelis-Menten analysis for deletion mutants show little changes in K_M-values, but indicate a decrease in k_{cat} upon removal of 2 helical turns of the connector helix.

Table 2
Michaelis-Menten analysis of USP7^{CD12345} constructs.

	k_{cat} (s^{-1})	K_M (μM)	k_{cat}/K_M ($\mu M^{-1}\ s^{-1}$)
WT	2.80 ± 0.04	8.80 ± 0.32	0.32
AQK552PGP	1.69 ± 0.02	8.48 ± 0.28	0.20
EAH560PGP	2.45 ± 0.03	9.47 ± 0.31	0.26
KR554AA R558A	1.10 ± 0.03	7.17 ± 0.54	0.15
KR554AE R558E	1.46 ± 0.05	9.75 ± 0.78	0.15
Δ538-541	2.47 ± 0.08	9.11 ± 0.86	0.27
Δ538-545	1.54 ± 0.09	11.86 ± 1.61	0.13
Δ561-564	2.87 ± 0.07	7.13 ± 0.39	0.40
Δ557-564	1.03 ± 0.02	6.04 ± 0.34	0.17

In the mutational analysis, both the charged patch, the rigidity and the length of the connector helix play a role in activation. Mutations in the helical element lead to a modest decrease in k_{cat}, but do not affect K_M. The observed effect is analogous to the changes seen in the presence of the allosteric activator GMPS, but in the opposite direction (Faesen et al., 2011; van der Knaap et al., 2005). In both cases the actual activation has not changed, but the equilibrium between the active and inactive state has shifted, in this case towards the inactive state. When this is disrupted, the equilibrium between active and inactive USP7 will shift as the efficiency of 'folding back' onto the CD of Ubl45 is somewhat disrupted (Fig. 4).

The HUBL domain has some flexibility on its own, as USP7 activity remains similar for the mutant EAH560PGP and upon removal of an α-helical turn on either side of the connector helix. Only upon tampering with the charge or removing multiple turns the activity drops to roughly half the k_{cat}. This suggests that the Ubl45 domain

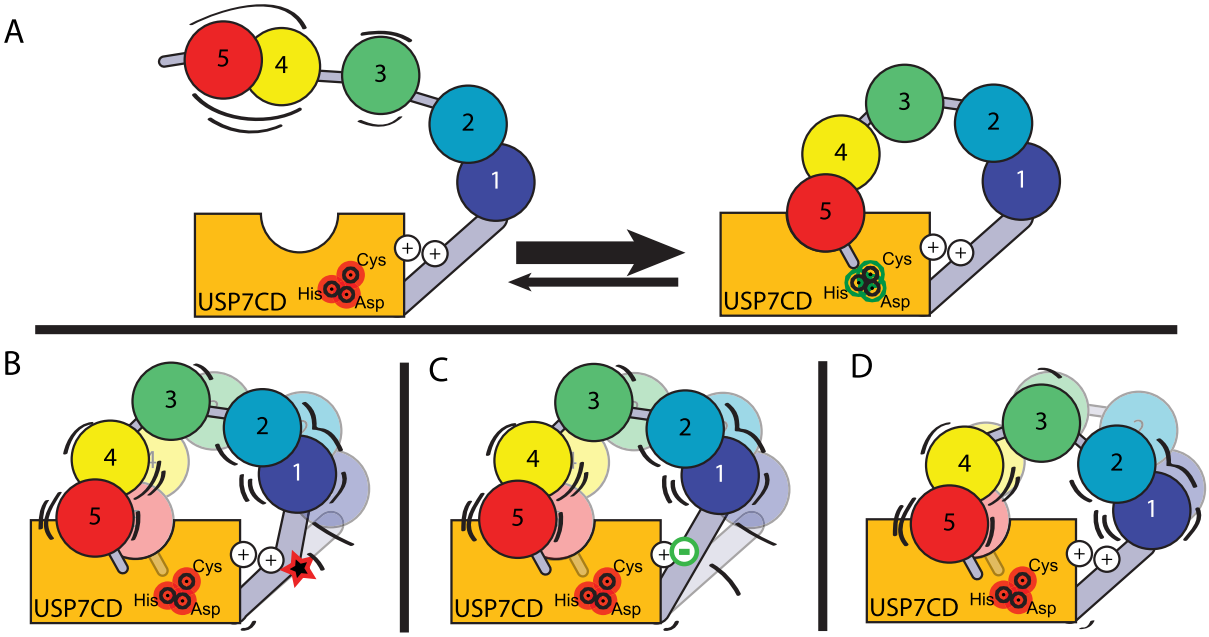

Fig. 4. Model of USP7 activation. (a) The model of USP7 self-activation shows an equilibrium between the inactive and active state, the transition requiring a rearrangement of the HUBL domain. (b) A bend within the connector helix of USP7 could change the efficiency of the positioning of Ubl45, affecting the overall activity of USP7. (c) Mutating the charged patch could have a similar effect, affecting the efficiency of the positioning of Ubl45 and thereby the USP7 self-activation. (d) Shortening of the connector helix with two helical turns affects the self-activation, possibly due to the efficiency of positioning of Ubl45.

is still able to activate the catalytic domain, albeit less efficiently. The exact positioning of Ubl45 is still unknown, but our mutational analysis shows that changes in the connector helix play a modest role in USP7 activity, probably by less efficient positioning of Ubl45.

We know that the linker regions of HUBL are rather flexible, as they are susceptible to proteolysis in protein purification. The first linker, between Ubl12 and Ubl3, can allow Ubl3 to make an angular motion of up to 35° (Pfoh et al., 2015), but most of the kinking should take place in the second linker, between Ubl3 and Ubl45. This second pivot point should allow for another 50° to get Ubl45 towards the CD. Distance-wise our structure shows that it can fit, but the exact interaction spot on the catalytic domain is not known.

Our structure begins to show the flexibility of the linker between Ubl12 and Ubl3, in line with recent co-crystal structures of (parts of) the HUBL domain with DNMT1 and ICP0 (Cheng et al., 2015; Pfoh et al., 2015). The relative bending of Ubl3 in these structures could have been induced by binding of the protein partner. In the USP7^{CD123} structure however, we don't have a binding partner, suggesting that USP7 does not need a specific modulator for this 'folding back' motion.

The HUBL domain is an important regulatory region in USP7. It contains the second binding site (Ubl12) of targets p53 and MDM, but where this interaction exactly takes place and whether this influences the activity on these targets is yet unknown. Ubl12 is known to bind GMPS, an allosteric activator, as well as DNMT1 (Cheng et al., 2015), URHF1 and ICP0 (Pfoh et al., 2015). The co-crystal structure of the Ubls with the ICP0 interactor peptide (4WPH; Pfoh et al., 2015) shows a similar bend of Ubl3 as we found in the structure of USP7^{CD123} and this is also seen in the structure of the full HUBL domain with DNMT1 (4YOC; Cheng et al., 2015). However, the Ubl45 in this structure has an extended conformation, and how 'closing' of the gap towards the catalytic domain occurs, an important step in USP7 self-activation, remains unclear.

The changes in k_{cat} observed upon mutation of the connector helix, and upon GMPS binding to Ubl123 (Faesen et al., 2011) indicate that these regions can be allosterically modulated. One could imagine that binding of small molecules at these sites could have a function in regulation of USP7 activity. As the charged patch of the connector helix is required for full activity, this could be a good starting point for structure-guided inhibitor design in a USP7 specific manner, especially as USP7 is emerging as an important drug target (Colland et al., 2009; Kessler, 2014; Lee et al., 2016; Nicholson and Suresh Kumar, 2011; Weinstock et al., 2012). Good understanding of the conformational changes and allosteric regulation of this critical DUB will be important to understand the effects of bound inhibitors. Our new structure will contribute to these efforts.

Acknowledgements

The authors would like to acknowledge the ESRF for their support, in particular beamline scientists at beamline 14-1. We thank the NKI protein facility for contributions to protein quality control experiments, Jonas Dörr and Hedwich Vlieg for assistance in the circular dichroism experiments, Robbie Joosten for help in refinement and Alexander Fish for critical discussion. KWF (NKI 2012-5398) and NWO Gravity project CGC.nl have contributed funding for this project.

Appendix A. Supplementary data

Supplementary data associated with this article can be found, in the online version, at http://dx.doi.org/10.1016/j.jsb.2016.05.005.

References

Alonso-de Vega, I., Martín, Y., Smits, V.A.J., 2014. USP7 controls Chk1 protein stability by direct deubiquitination. Cell Cycle 13, 3921–3926.
Brooks, C.L., Gu, W., 2006. P53 ubiquitination: Mdm2 and beyond. Mol. Cell 21, 307–315.
Cheng, J., Yang, H., Fang, J., Ma, L., Gong, R., Wang, P., Li, Z., Xu, Y., 2015. Molecular mechanism for USP7-mediated DNMT1 stabilization by acetylation. Nat. Commun. 6, 7023.
Clague, M.J., Coulson, J.M., Urbé, S., 2012. Cellular functions of the DUBs. J. Cell Sci. 125, 277–286.

Clague, M.J., Barsukov, I., Coulson, J.M., Liu, H., Rigden, D.J., Urbé, S., 2013. Deubiquitylases from genes to organism. Physiol. Rev. 93, 1289–1315.
Clerici, M., Luna-Vargas, M.P.A., Faesen, A.C., Sixma, T.K., 2014. The DUSP-Ubl domain of USP4 enhances its catalytic efficiency by promoting ubiquitin exchange. Nat. Commun. 5, 5399.
Colland, F., Formstecher, E., Jacq, X., Reverdy, C., Planquette, C., Conrath, S., Trouplin, V., Bianchi, J., Aushev, V.N., Camonis, J., Calabrese, A., Borg-Capra, C., Sippl, W., Collura, V., Boissy, G., Rain, J.-C., Guedat, P., Delansorne, R., Daviet, L., 2009. Small-molecule inhibitor of USP7/HAUSP ubiquitin protease stabilizes and activates p53 in cells. Mol. Cancer Ther. 8, 2286–2295.
Cummins, J.M., Rago, C., Kohli, M., Kinzler, K.W., Lengauer, C., Vogelstein, B., 2004. Tumour suppression: disruption of HAUSP gene stabilizes p53. Nature 428, 1–486.
Davis, I.W., Murray, L.W., Richardson, J.S., Richardson, D.C., 2004. MOLPROBITY: structure validation and all-atom contact analysis for nucleic acids and their complexes. Nucleic Acids Res. 32, W615-9.
Du, Z., Song, J., Wang, Y., Zhao, Y., Guda, K., Yang, S., Kao, H.-Y., Xu, Y., Willis, J., Markowitz, S.D., Sedwick, D., Ewing, R.M., Wang, Z., 2010. DNMT1 stability is regulated by proteins coordinating deubiquitination and acetylation-driven ubiquitination. Sci. Signal. 3, ra80.
Emsley, P., Lohkamp, B., Scott, W.G., Cowtan, K., 2010. Features and development of Coot. Acta Crystallogr. D Biol. Crystallogr. 66, 486–501.
Epping, M.T., Meijer, L.A.T., Krijgsman, O., Bos, J.L., Pandolfi, P.P., Bernards, R., 2011. TSPYL5 suppresses p53 levels and function by physical interaction with USP7. Nat. Cell Biol. 13, 102–108.
Everett, R.D., Meredith, M., Orr, A., Cross, A., Kathoria, M., Parkinson, J., 1997. A novel ubiquitin-specific protease is dynamically associated with the PML nuclear domain and binds to a herpesvirus regulatory protein. EMBO J. 16, 1519–1530.
Faesen, A.C., Dirac, A.M.G., Shanmugham, A., Ovaa, H., Perrakis, A., Sixma, T.K., 2011. Mechanism of USP7/HAUSP activation by its C-terminal ubiquitin-like domain and allosteric regulation by GMP-synthetase. Mol. Cell 44, 147–159.
Faustrup, H., Bekker-Jensen, S., Bartek, J., Lukas, J., Mailand, N., 2009. USP7 counteracts SCFbetaTrCP- but not APCCdh1-mediated proteolysis of Claspin. J. Cell Biol. 184, 13–19.
Fernández-Montalván, A., Bouwmeester, T., Joberty, G., Mader, R., Mahnke, M., Pierrat, B., Schlaeppi, J.-M., Worpenberg, S., Gerhartz, B., 2007. Biochemical characterization of USP7 reveals post-translational modification sites and structural requirements for substrate processing and subcellular localization. FEBS J. 274, 4256–4270.
Hao, Y.-H., Fountain, M.D., Fon Tacer, K., Xia, F., Bi, W., Kang, S.-H.L., Patel, A., Rosenfeld, J.A., Le Caignec, C., Isidor, B., Krantz, I.D., Noon, S.E., Pfotenhauer, J.P., Morgan, T.M., Moran, R., Pedersen, R.C., Saenz, M.S., Schaaf, C.P., Potts, P.R., 2015. USP7 acts as a molecular rheostat to promote WASH-dependent endosomal protein recycling and is mutated in a human neurodevelopmental disorder. Mol. Cell 59, 956–969.
Hershko, A., Ciechanover, A., 1998. The ubiquitin system. Annu. Rev. Biochem. 67, 425–479.
Hicke, L., Dunn, R., 2003. Regulation of membrane protein transport by ubiquitin and ubiquitin-binding proteins. Annu. Rev. Cell Dev. Biol. 19, 141–172.
Holowaty, M.N., Frappier, L., 2004. HAUSP/USP7 as an Epstein-Barr virus target. Biochem. Soc. Trans. 32, 731–732.
Holowaty, M.N., Sheng, Y., Nguyen, T., Arrowsmith, C., Frappier, L., 2003. Protein interaction domains of the ubiquitin-specific protease, USP7/HAUSP. J. Biol. Chem. 278, 47753–47761.
Hu, M., Li, P., Li, M., Li, W., Yao, T., Wu, J.-W., Gu, W., Cohen, R.E., Shi, Y., 2002. Crystal structure of a UBP-family deubiquitinating enzyme in isolation and in complex with ubiquitin aldehyde. Cell 111, 1041–1054.
Hussain, S., Zhang, Y., Galardy, P., 2009. DUBs and cancer. Cell Cycle 8, 1688–1697.
Joosten, R.P., Long, F., Murshudov, G.N., Perrakis, A., 2014. The PDB_REDO server for macromolecular structure model optimization. IUCrJ 1, 213–220.
Kabsch, W., 2010. XDS. Acta Crystallogr. D. Biol. Crystallogr. 66, 125–132.
Kessler, B.M., 2014. Selective and reversible inhibitors of ubiquitin-specific protease 7: a patent evaluation (WO2013030218).
Komander, D., Rape, M., 2012. The ubiquitin code. Annu. Rev. Biochem. 81, 203–229.
Komander, D., Clague, M.J., Urbé, S., 2009. Breaking the chains: structure and function of the deubiquitinases. Nat. Rev. Mol. Cell Biol. 10, 550–563.
Lecona, E., Narendra, V., Reinberg, D., 2015. USP7 cooperates with SCML2 to regulate the activity of PRC1. Mol. Cell. Biol.
Lee, G., Oh, T.-I., Um, K.B., Yoon, H., Son, J., Kim, B.M., Kim, H.-I., Kim, H., Kim, Y.J., Lee, C.-S., Lim, J.-H., 2016. Small-molecule inhibitors of USP7 induce apoptosis through oxidative and endoplasmic reticulum stress in cancer cells. Biochem. Biophys. Res. Commun. 470, 181–186.
Li, M., Chen, D., Shiloh, A., Luo, J., Nikolaev, A.Y., Qin, J., Gu, W., 2002. Deubiquitination of p53 by HAUSP is an important pathway for p53 stabilization. Nature 416, 648–653.
Ma, J., Martin, J.D., Xue, Y., Lor, L.A., Kennedy-Wilson, K.M., Sinnamon, R.H., Ho, T.F., Zhang, G., Schwartz, B., Tummino, P.J., Lai, Z., 2010. C-terminal region of USP7/HAUSP is critical for deubiquitination activity and contains a second mdm2/p53 binding site. Arch. Biochem. Biophys. 503, 207–212.
McCoy, A.J., Grosse-Kunstleve, R.W., Adams, P.D., Winn, M.D., Storoni, L.C., Read, R.J., 2007. Phaser crystallographic software. J. Appl. Crystallogr. 40, 658–674.
Murshudov, G.N., Skubák, P., Lebedev, A.A., Pannu, N.S., Steiner, R.A., Nicholls, R.A., Winn, M.D., Long, F., Vagin, A.A., 2011. REFMAC5 for the refinement of macromolecular crystal structures. Acta Crystallogr. D Biol. Crystallogr. 67, 355–367.
Nanduri, B., Suvarnapunya, A.E., Venkatesan, M., Edelmann, M.J., 2013. Deubiquitinating enzymes as promising drug targets for infectious diseases. Curr. Pharm. Des. 19, 3234–3247.
Nicholls, R.A., Fischer, M., McNicholas, S., Murshudov, G.N., 2014. Conformation-independent structural comparison of macromolecules with ProSMART. Acta Crystallogr. D Biol. Crystallogr. 70, 2487–2499.
Nicholson, B., Suresh Kumar, K.G., 2011. The multifaceted roles of USP7: new therapeutic opportunities. Cell Biochem. Biophys. 60, 61–68.
Nijman, S.M.B., Luna-Vargas, M.P.A., Velds, A., Brummelkamp, T.R., Dirac, A.M.G., Sixma, T.K., Bernards, R., 2005. A genomic and functional inventory of deubiquitinating enzymes. Cell 123, 773–786.
Passmore, L.A., Barford, D., 2004. Getting into position: the catalytic mechanisms of protein ubiquitylation. Biochem. J. 379, 513–525.
Pfoh, R., Lacdao, I.K., Georges, A.A., Capar, A., Zheng, H., Frappier, L., Saridakis, V., 2015. Crystal structure of USP7 ubiquitin-like domains with an ICP0 peptide reveals a novel mechanism used by viral and cellular proteins to target USP7. PLoS Pathog. 11, e1004950.
Pickart, C.M., 2001. Mechanisms underlying ubiquitination. Annu. Rev. Biochem. 70, 503–533.
Reyes-Turcu, F.E., Ventii, K.H., Wilkinson, K.D., 2009. Regulation and cellular roles of ubiquitin-specific deubiquitinating enzymes. Annu. Rev. Biochem. 78, 363–397.
Sahtoe, D.D., Sixma, T.K., 2015. Layers of DUB regulation. Trends Biochem. Sci. 40, 456–467.
Saridakis, V., Sheng, Y., Sarkari, F., Holowaty, M.N., Shire, K., Nguyen, T., Zhang, R.G., Liao, J., Lee, W., Edwards, A.M., Arrowsmith, C.H., Frappier, L., 2005. Structure of the p53 binding domain of HAUSP/USP7 bound to Epstein-Barr nuclear antigen 1 implications for EBV-mediated immortalization. Mol. Cell 18, 25–36.
Schwertman, P., Vermeulen, W., Marteijn, J.A., 2013. UVSSA and USP7, a new couple in transcription-coupled DNA repair. Chromosoma.
Shabek, N., Ciechanover, A., 2010. Degradation of ubiquitin: the fate of the cellular reaper. Cell Cycle 9, 523–530.
Sheng, Y., Saridakis, V., Sarkari, F., Duan, S., Wu, T., Arrowsmith, C.H., Frappier, L., 2006. Molecular recognition of p53 and MDM2 by USP7/HAUSP. Nat. Struct. Mol. Biol. 13, 285–291.
Song, M.S., Salmena, L., Carracedo, A., Egia, A., Lo-Coco, F., Teruya-Feldstein, J., Pandolfi, P.P., 2008. The deubiquitinylation and localization of PTEN are regulated by a HAUSP-PML network. Nature 455, 813–817.
Sowa, M.E., Bennett, E.J., Gygi, S.P., Harper, J.W., 2009. Defining the human deubiquitinating enzyme interaction landscape. Cell 138, 389–403.
Streich, F.C., Lima, C.D., 2014. Structural and functional insights to ubiquitin-like protein conjugation. Annu. Rev. Biophys. 43, 357–379.
Studier, F.W., 2005. Protein production by auto-induction in high density shaking cultures. Protein Expr. Purif. 41, 207–234.
Todi, S.V., Paulson, H.L., 2011. Balancing act: deubiquitinating enzymes in the nervous system. Trends Neurosci. 34, 370–382.
van der Horst, A., de Vries-Smits, A.M.M., Brenkman, A.B., van Triest, M.H., van den Broek, N., Colland, F., Maurice, M.M., Burgering, B.M.T., 2006. FOXO4 transcriptional activity is regulated by monoubiquitination and USP7/HAUSP. Nat. Cell Biol. 8, 1064–1073.
van der Knaap, J.A., Kumar, B.R.P., Moshkin, Y.M., Langenberg, K., Krijgsveld, J., Heck, A.J.R., Karch, F., Verrijzer, C.P., 2005. GMP synthetase stimulates histone H2B deubiquitylation by the epigenetic silencer USP7. Mol. Cell 17, 695–707.
Varshavsky, A., 2012. The ubiquitin system, an immense realm. Annu. Rev. Biochem. 81, 167–176.
Weinstock, J., Wu, J., Cao, P., Kingsbury, W.D., McDermott, J.L., Kodrasov, M.P., McKelvey, D.M., Suresh Kumar, K.G., Goldenberg, S.J., Mattern, M.R., Nicholson, B., 2012. Selective dual inhibitors of the cancer-related deubiquitylating proteases USP7 and USP47. ACS Med. Chem. Lett. 3, 789–792.
Winn, M.D., Ballard, C.C., Cowtan, K.D., Dodson, E.J., Emsley, P., Evans, P.R., Keegan, R.M., Krissinel, E.B., Leslie, A.G.W., McCoy, A., McNicholas, S.J., Murshudov, G.N., Pannu, N.S., Potterton, E.A., Powell, H.R., Read, R.J., Vagin, A., Wilson, K.S., 2011. Overview of the CCP4 suite and current developments. Acta Crystallogr. D Biol. Crystallogr. 67, 235–242.
Wrigley, J.D., Eckersley, K., Hardern, I.M., Millard, L., Walters, M., Peters, S.W., Mott, R., Nowak, T., Ward, R.A., Simpson, P.B., Hudson, K., 2011. Enzymatic characterisation of USP7 deubiquitinating activity and inhibition. Cell Biochem. Biophys. 60, 99–111.
Zhu, Q., Sharma, N., He, J., Wani, G., Wani, A.A., 2015. USP7 deubiquitinase promotes ubiquitin-dependent DNA damage signaling by stabilizing RNF168.